# The Inverse Problem of Electrical Capacitance Tomography and its Application to Gas-Oil 2-Phase Flow Imaging

ANDRES FRAGUELA
Facultad de Ciencias Fisico Matematicas
Benemerita Universidad Autonoma de Puebla
Av San Claudio y Rio Verde, Col San Manuel, Ciudad Universitaria, Pueble, Puebla, 72570
MEXICO

CARLOS GAMIO
Instituto Mexicano del Petroleo
Eje Central L Cardenas Nte #152, Col San Bartolo Atepehuacan, Mexico, DF, 07730
MEXICO

DORIS HINESTROZA
Departamento de Matematicas
Universidad del Valle
Cali, Valle del Cauca, A.A. 25360
COLOMBIA

*Abstract:* - Electrical-capacitance tomography (ECT) is a novel technique for the non-invasive internal visualization of industrial processes such as mixing, separation and multiphase flow, involving electrically non-conducting mixtures. One of the most promising potential applications of ECT is the determination of the amount of gas, oil and water produced by an oil well. The principle of ECT is to place a ring of between 8 and 16 adjacent electrodes (known as the sensor) around a particular cross-section of the process vessel or pipe (which must have insulating walls in that area), and to measure all the inter-electrode capacitances. The measurements are then used to generate an image of the electrical permittivity variations (reflecting the mixture composition) inside the sensor through a suitable inversion algorithm. In this work, a new algorithm based on a set of integral equations, which are equivalent to the differential model formulation, is presented. Using this integral relationships, the problem of identifying the unknown permittivity reduces to solving a quadratic optimization problem with quadratic constraints, for the coefficients of the expansion of the permittivity with respect to an orthonormal base conveniently chosen in a Sobolev space of functions defined in the sensor cross-section.

*Key-Words:* - Electrical Tomography, Capacitance, Inversion Algorithm, Imaging, Two-Phase Flow

## 1 Introduction

Oil wells typically produce not just oil, but a complex multiphase mixture having variable amounts of oil, gas and water. The determination of the quantity of each component actual being produced by each specific well is of the greatest importance for the efficient exploitation of the reservoirs. The conventional way of doing this is by separating the mixture and measuring each individual component using single-phase flowmeters. However, the three-phase separators needed are excessively bulky and expensive. As an alternative, multiphase flow measurement techniques that do not require mixture separation have emerged in the last decade [7]. Among the most promising approaches currently under investigation is one based on multiphase flow visualization using tomographic methods [2], in particular electrical-capacitance tomography (ECT). The main advantage of the tomographic methods lies in their inherently non-invasive and flow-regime independent operation.

ECT is an emerging technique aimed at the non-invasive internal visualization of electrically non-conducting mixtures in industrial processes like mixing, separation and multiphase flow [10,11]. Only the application to flow imaging will be considered here. The basic principle of this method is to place a sensor containing an array of between 8 and 16 contiguous sensing electrodes around the pipe carrying the process fluids, at the cross-section to be investigated (see figs. 1 and 2). The pipe wall should be electrically non-conducting in the zone of the

electrodes. The electrodes are typically 10 cm long. The sensor also has a couple of cylindrical end guards adjacent to the electrodes and an outer cylindrical metallic screen (not shown in fig.1) covering the whole thing, all of which are always kept at an electric potential of zero volts. The sensing electrodes are connected to an apparatus that allows all the mutual capacitances between the different electrode pairs to be measured, and from this set of measurements the electrical permittivity distribution inside the sensor is obtained using a suitable inversion algorithm. The permittivity distribution reflects the spatial arrangement of the phases in the flow. Image reconstruction can thus be regarded as an inverse permittivity problem.

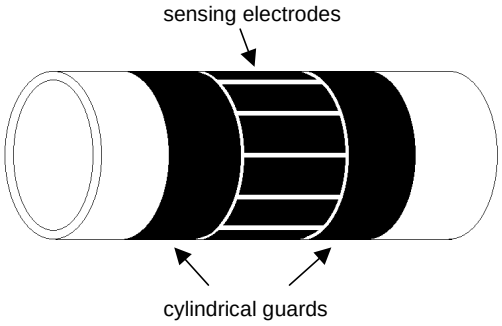


Fig.1 12-electrode sensor

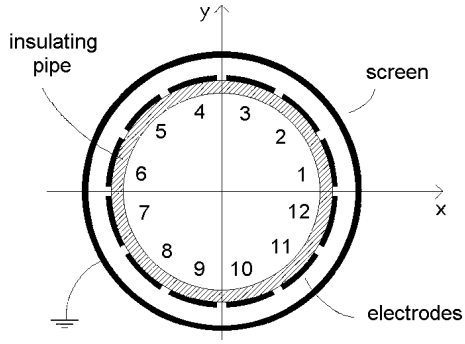


Fig.2 Cross-section of sensor

For 2-phase flows like gas-oil, the permittivity distribution directly determines the distribution of each phase, whereas for 3-phase ones like gas-oil-water, the distribution of an additional parameter (i.e. conductivity, etc.) must be obtained first through a different tomographic modality in order to resolve each phase distribution.

To measure the mutual capacitance $C_{i,j}$ between electrodes *i* and *j*, a sinusoidal voltage of magnitude *V* is applied to electrode *i* (source) keeping the rest at zero potential, and the charge *Q* induced on electrode *j* (detector) is measured. $C_{i,j}$ is then given by

$$C_{i,j} = \frac{V_i}{Q_j} \qquad (1)$$

Because $C_{i,j} = C_{j,i}$, there are only $n = \frac{1}{2} N (N - 1)$ independent mutual capacitance values, where *N* is the number of electrodes. For a 12-electrode sensor $n = 66$.

The use of the cylindrical guards at the ends of the sensing electrodes (and assuming that the phase distribution changes slowly in the axial direction) allows the sensor to be represented by a two-dimensional (2-D) model [8] like the one shown in fig.2. Assuming that the flow changes negligibly during the time required for one set of 66 measurements, and that the frequency of the excitation voltage is so small that the corresponding wavelength is much larger than the sensor dimensions, a static model can be considered.

# 2 Problem Formulation

The forward problem is to determine the mutual capacitances $C_{i,j}$ given a known permittivity distribution inside the pipe. The inverse problem involves finding an unknown permittivity distribution inside the pipe based on the knowledge of all the $\frac{1}{2} N (N - 1)$ mutual capacitances $C_{i,j}$ (note that in the pipe itself and in the area between the pipe and the screen the permittivity distribution is known).

## 2.1 Mathematical model

The sensor is modeled (fig.3) as a dielectric region $\Omega$ made of three subregions: a circle $\Omega_1$ and two adjacent concentric rings $\Omega_2$ and $\Omega_3$, representing the interior of the pipe, the pipe wall and the area between the pipe and the screen, respectively. The electrodes, being very thin and having very small gaps between them, are modeled as equipotential surfaces (lines in the 2-D model) covering the entire boundary between $\Omega_2$ and $\Omega_3$. The screen is modeled as an equipotential line on the outer perimeter of $\Omega_3$.

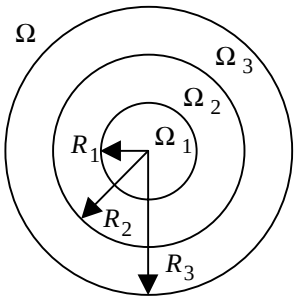


Fig.3 Sensor model

Mathematically we have $\Omega = \Omega_1 \cup \Omega_2 \cup \Omega_3$ where

$$\Omega_1 = \{z = (x,y) : |z| < R_1 \} \quad (2)$$

$$\Omega_2 = \{z = (x,y) : R_1 < |z| < R_2 \} \quad (3)$$

$$\Omega_3 = \{z = (x,y) : R_2 < |z| < R_3 \} \quad (4)$$

Each one of the subregions $\Omega_i$ ($i$ = 1,2,3) has an electrical permittivity $\varepsilon_i(x,y)$. For $i$ = 2,3 the function $\varepsilon_i(x,y)$ has a known constant value $\varepsilon_i$, whereas it is unknown for $i$ = 1.

We shall consider that electrode $i$ lies on the arch $S_i$ defined by

$$S_i = \{z=(x,y) : |z| = R_2,\ 2\pi(i\text{-}1)/N \le \arg(z) \le 2\pi i/N \} \quad (5)$$

We shall denote by $V^{(i)}(x,y)$, $i$ = 1,2,..,$N$, the potential produced in $\Omega$ when

$$V^{(i)}(x,y) = \begin{cases} 0 \ \text{ in } \ |z| = R_3 \\ 1 \ \text{ in } \ |z| \in S_i \\ 0 \ \text{ in } \ |z| = R_2, \ \ z \notin S_i \end{cases} \quad (6)$$

and also $\varepsilon(x,y) = \varepsilon_j(x,y)$ if $(x,y) \in \Omega_j$ ($j$ = 1,2,3) and $\varepsilon_j(x,y)$ is constant $\varepsilon_j$ for $j$ = 2,3.

We shall suppose that

$V_j^{(i)}(x,y) = V^{(i)}(x,y)$ if $(x,y) \in \Omega_j$ ($j$ = 1,2,3).

In this case, for $V_1^{(i)}(x,y)$, $V_2^{(i)}(x,y)$ and $V_3^{(i)}(x,y)$ we have that

$$\nabla(\varepsilon_1(x,y)\nabla V_1^{(i)}) = 0 \ \text{ in } \ |z| < R_1 \quad (7)$$

$$\Delta V_2^{(i)} = 0 \ \text{ in } \ R_1 < |z| < R_2 \quad (8)$$

$$\Delta V_3^{(i)} = 0 \ \text{ in } \ R_2 < |z| < R_3 \quad (9)$$

that satisfy the boundary conditions

$$V_1^{(i)}(z) = V_2^{(i)}(z) \quad (10)$$

$$\varepsilon_1(x,y)\frac{\partial V_1^{(i)}}{\partial n_1}(z) = \varepsilon_2 \ \frac{V_2^{(i)}}{\partial n_1}(z) \quad (11)$$

on $|z| = R_1$, where $n_1$ is the exterior normal unitary vector to the circle $|z| = R_1$.

Additionally to equations (8) and (9), we have

$$V_2^{(i)}(x,y) = \begin{cases} 1 \ \text{ in } \ |z| \in S_i \\ 0 \ \text{ in } \ |z| = R_2, \ \ z \notin S_i \end{cases} \quad (12)$$

$$V_3^{(i)}(x,y) = \begin{cases} 0 \ \text{ in } \ |z| = R_3 \\ 1 \ \text{ in } \ |z| \in S_i \\ 0 \ \text{ in } \ |z| = R_2, \ \ z \notin S_i \end{cases} \quad (13)$$

## 2.2 The inverse problem

In what follows, our model will be determined by the boundary value problem (7) - (13). We can describe the inverse problem as follows:

*Given* ½ $N$ ($N$ - 1) *values* $C_{i,j}$ ($i, j$ = 1,2,…,$N$) ($i < j$), *of the mutual capacitances between the electrodes* $S_i$ *and* $S_j$, *determine approximately the value of* $\varepsilon_1(x,y)$ *using the model (7) - (13).*

This problem is called inverse of the direct problem that consists in calculating the solution $V^{(i)}(x,y)$ of the boundary value problem (7) - (13) and the mutual capacitance values $C_{i,j}$, for a known permittivity $\varepsilon_1(x,y)$.

The direct problem is a well posed problem in the Hadamard sense and is numerically stable [4], but the inverse problem is an ill posed problem and is numerically unstable. In fact, if we don't have a regularized algorithm [3] for the reconstruction of $\varepsilon_1(x,y)$, small errors in the data may produce a large error in the reconstructed solution. On the other hand, the numerical discretization of the problem can also lead to significant deviations in the calculation of $\varepsilon_1(x,y)$. We will propose an algorithm that will take into account the ill-posedness and the numerical instability in the solution of the inverse problem.

The mutual capacitance values are given by

$$C_{i,j} = K \int_{S_j} \varepsilon(x,y) \frac{\partial V^{(i)}}{\partial n_2} ds \quad (14)$$

where $n_2$ is the exterior normal unitary vector to the circle $|z| = R_2$ and $K$ is a constant with units of inverse potential.

We shall observe that is possible to obtain from (14) the relation

$$\int_{S_j^-} \frac{\partial V_2^{(i)}}{\partial n_2} ds = \frac{1}{\varepsilon_2} \left\{ \varepsilon_3 \int_{S_j^+} \frac{\partial V_3^{(i)}}{\partial n_2} ds - \frac{C_{i,j}}{K} \right\} \quad (15)$$

where $S_j^-$ and $S_j^+$ denote the arc of $S_j$ intercepted with the domains $\overline{\Omega}_3$ y $\overline{\Omega}_2$ respectively.

The fact that the function $V_3^{(i)}$ is decoupled in the model (7) - (13) and satisfies the Dirichlet problem given by (9) and (13), means that we can calculate $V_3^{(i)}$ independently, which allows us to obtain the value of the right-hand side of (15) from the knowledge of the mutual capacitance values measured experimentally $C_{i,j}$. For that reason we will denote

$$c_{i,j} = \int_{S_j^-} \frac{\partial V_2^{(i)}}{\partial n_2} ds \quad (16)$$

We will consider an equivalent problem to the inverse problem as follows:

*Given* ½ $N$ ($N$ - 1) *values* $c_{i,j}$ ($i, j$ = 1,2,…,$N$) ($i < j$), *obtained using* (15) *and* (16), *determine approximately the value of* $\varepsilon_1(x,y)$ *using the model (7) - (13).*

## 3 Problem Solution

From now on we will consider that the solution $V_3^{(i)}$ is known. In the scheme to the solution we will introduce several auxiliary functions whose analytical or numerical calculation can be constructed independently.

### 3.1 Fundamental Relations

To construct the algorithm for the solution of the inverse problem we have first to find a set a relations between the functions $V_1^{(i)}$, $V_2^{(i)}$ and $\varepsilon_1$, that allows to obtain $\varepsilon_1$ approximately from the data $\{c_{i,j}\}$, $i, j = 1,2,\ldots,N$, $(i<j)$ given by (15) and (16).

We will classify the relations in two different types:

(a) Those that allow us to obtain $V_2^{(i)}$ and $\dfrac{\partial V_2^{(i)}}{\partial n_2}$ in $|\xi| = R_1$ from the data $\{c_{i,j}\}$ and the calculation of $V_3^{(i)}$, and also ensure that $V_2^{(i)}$ and $\dfrac{\partial V_2^{(i)}}{\partial n_2}$ in $|\xi| = R_1$ are the restriction of a harmonic function in $\Omega_2$ that satisfies the boundary conditions (12) in $|\xi| = R_2$.

(b) Those that allow us to obtain simultaneously $V_1^{(i)}$, $\nabla V_1^{(i)}$ and $\varepsilon_1$ of an approximately manner from the minimization of a objective functional in such way as to satisfy equation (7) and the boundary conditions (11) and (10), taking into account the *a priory* information that we have about $\varepsilon_1(x,y)$ in terms of bounds.

If we apply Green's formula to the Laplace operator in $\Omega_2$ and the functions $V_2^{(i)}(\xi)$ and $N(z,\xi)$, where

$$\Delta N(z,\xi) = \delta(z-\xi); \qquad z,\xi \in \Omega_2 \quad (17)$$

$$\frac{\partial N}{\partial n_z}(z,\xi) = 0 \quad \text{in} \quad |z| = R_1, \quad \xi \in \Omega_2 \quad (18)$$

$$N(z,\xi) = 0 \quad \text{in} \quad |z| = R_2, \quad \xi \in \Omega_2 \quad (19)$$

$\delta(z-\xi)$ being a Dirac's delta function, and we take the limit when $z \to z_o$ with $|z_o| = R_1$, then we obtain for $i = 1,2,\ldots,N$

$$V_2^{(i)}(z_o) = \int_{|\xi|=R_1} N(z_o,\xi)\frac{\partial V_2^{(i)}}{\partial n_1}(\xi)ds_\xi + \int_{S_i}\frac{\partial N}{\partial n_2}(z_o,\xi_1)ds_{\xi_1} \quad (20)$$

where $|\xi| = R_1$ and $|\xi_1| = R_2$, which express the relation that must exist between the boundary values of a harmonic function in $\Omega_2$ and its normal derivative in $|\xi| = R_1$, for the boundary condition (12) to be satisfied in $|\xi_1| = R_2$.

Now, we consider the boundary problem

$$\nabla(\varepsilon_1(x,y)\nabla V_1^{(i)}) = 0 \quad \text{in} \quad |z| < R_1$$

$$\varepsilon_1(x,y)\frac{\partial V_1^{(i)}}{\partial n_1}(z) = \Psi \quad \text{in} \quad |z| = R_1$$

with

$$\int_{|\xi|=R_1}\Psi ds = 0.$$

Making the change of variables

$$\varepsilon_1(x,y)\nabla V_1^{(i)} = \nabla u^{(i)}, \quad (21)$$

then $u^{(i)}$ satisfies the boundary problem

$$\Delta u^{(i)} = 0 \quad \text{in} \quad |z| < R_1$$

$$\frac{\partial u^{(i)}}{\partial n_1}(z) = \Psi \quad \text{in} \quad |z| = R_1,$$

this solution is represented by

$$u^{(i)}(z) = -\frac{1}{\pi}\int_{|\xi|=R_1}\Psi(\xi)\ln|\xi - z|ds_\xi + const, \quad (22)$$

with $|z| < R_1$.

From (21) and (22) and the boundary conditions (11) we obtain

$$\varepsilon_1(z)\nabla V_1^{(i)}(z) = -\frac{\varepsilon_2}{\pi}\int_{|\xi|=R_1}\frac{\partial V_2^{(i)}}{\partial n_1}(\xi)\nabla_z \ln|\xi - z|ds_\xi \quad (23)$$

with $|z| < R_1$.

If we apply Green's formula to the function $V_1^{(i)}$ and any $C^{(2)}(|z| < R_1)$ function we have

$$\int_{|\xi|<R_1}\left\{v\nabla(\varepsilon_1(\xi)\nabla V_1^{(i)}) - V_1^{(i)}\Delta v\right\}d\xi = \quad (24)$$

$$\int_{|\xi|<R_1}(\varepsilon_1 - 1)\nabla V_1^{(i)}\cdot\nabla v d\xi - \int_{|\xi|=R_1}\left(v\varepsilon_1\frac{\partial V_1^{(i)}}{\partial n_1}(\xi) - V_1^{(i)}\frac{\partial v}{\partial n_1}\right)ds_\xi$$

If instead of $v$ in (24) we take the Green's functions

$$d(z,\xi) = -\frac{1}{4\pi}\ln\left(\frac{R_1^2 - 2\rho r\cos(t-\tau) + \rho^2 r^2 R_1^{-2}}{r^2 - 2\rho r\cos(t-\tau) + \rho^2}\right)$$

and

$$n(z,\xi)=\frac{1}{2\pi}\ln\left(r^2-2\rho r\cos(t-\tau)+\rho^2\right)$$
$$+\frac{1}{2\pi}\ln\left(\frac{R_1^{\,4}}{\rho^2}-2\frac{R_1^2 r}{\rho}\cos(t-\tau)+r^2\right)-\frac{1}{\pi}\ln\left(\frac{R_1}{\rho}\right)$$

that correspond to the Dirichlet and Neumann problems in $|z|<R_1$, and taking into account relations (20) and (23) we have

$$V_1^{(i)}(z)=\int_{|\xi|<R_1}\nabla V_1^{(i)}(\xi)\cdot\nabla_\xi d(z,\xi)d\xi + \int_{|\varphi|=R_1}F(z,\varphi)\frac{\partial V_2^{(i)}}{\partial n_1}(\varphi)ds_\varphi+h_i(z) \tag{25}$$

$$V_1^{(i)}(z)=\int_{|\xi|<R_1}\nabla V_1^{(i)}(\xi)\cdot\nabla_\xi n(z,\xi)d\xi + \int_{|\varphi|=R_1}G(z,\varphi)\frac{\partial V_2^{(i)}}{\partial n_1}(\varphi)ds_\varphi+a_i \tag{26}$$

where

$$F(z,\varphi)=\frac{\varepsilon_2}{\pi}\int_{|\xi|<R_1}\nabla_\xi\ln|\xi-\varphi\cdot|\nabla_\xi d(z,\xi)d\xi - \int_{|\psi|=R_1}N(\psi,\varphi)\frac{\partial d}{\partial n_\psi}(z,\psi)ds_\psi, \tag{27}$$

$$G(z,\varphi)=\frac{\varepsilon_2}{\pi}\int_{|\xi|<R_1}\nabla_\xi\ln|\xi-\varphi\cdot|\nabla_\xi n(z,\xi)d\xi +\varepsilon_2 n(z,\varphi)-\frac{1}{2\pi R_1}\int_{|\psi|=R_1}N(\psi,\varphi)ds_\psi, \tag{28}$$

$$h_{(i)}(z)=-\int_{S_i}\left\{\int_{|\psi|=R_1}\frac{\partial d}{\partial n_\psi}(z,\psi)\frac{\partial N}{\partial n_{\xi_1}}(\psi,\xi_1)ds_\psi\right\}ds_{\xi_1} \tag{29}$$

and

$$a_i=-\frac{1}{2\pi R_1}\int_{S_i}\left\{\int_{|\psi|=R_1}\frac{\partial N}{\partial n_{\xi_1}}(\psi,\xi_1)ds_\psi\right\}ds_{\xi_1} \tag{30}$$

Relation (20) is of type **a**, whereas (23), (25) and (26) are relations of type **b**.

## 3.1 Algorithm for the solution the inverse problem

### 3.1.1 Step 1

The function $V_2^{(i)}$ can be written as the Fourier series:

$$V_2^{(i)}(r,\theta)=a_o^{(i)}+b_o^{(i)}\ln r+\sum_{n=1}^{\infty}(a_n^{(i)}r^n+b_n^{(i)}r^{-n})\cos(n\theta)+\sum_{n=1}^{\infty}(c_n^{(i)}r^n+d_n^{(i)}r^{-n})\sin(n\theta) \tag{31}$$

From equation (31) we can obtain the Fourier series for $\frac{\partial V_2^{(i)}}{\partial n_1}(\xi)$ in $|\xi|=R_1$. Applying the boundary conditions (12) and using the data (16), the coefficients in (31) are given by the relations:

$$a_o^{(i)}+b_o^{(i)}\ln R_2=1/N,\quad i=1,...,N \text{ and } k=0 \tag{32}$$

$$a_k^{(i)}R_2^{\,k}+b_k^{(i)}R_2^{\,-k}=\frac{\sin\left(\frac{2\pi ik}{N}\right)-\sin\left(\frac{2\pi(i-1)k}{N}\right)}{\pi k} \tag{33}$$

$$c_k^{(i)}R_2^{\,k}+d_k^{(i)}R_2^{\,-k}=\frac{\cos\left(\frac{2\pi(i-1)k}{N}\right)-\cos\left(\frac{2\pi ik}{N}\right)}{\pi k} \tag{34}$$

$$i=1,\cdots,N;\qquad k\ge 1,$$

$$c_{i,j}=\frac{2\pi}{N}b_o^{(i)}+\sum_{n=1}^{\infty}\left[\left(2a_n^{(i)}R_2^n-\frac{\sin\left(\frac{2\pi in}{N}\right)-\sin\left(\frac{2\pi(i-1)n}{N}\right)}{\pi n}\right)\cdot\left(\sin\left(\frac{2\pi jn}{N}\right)-\sin\left(\frac{2\pi(j-1)n}{N}\right)\right)\right]+\sum_{n=1}^{\infty}\left(2c_n^{(i)}R_2^n-\frac{\cos\left(\frac{2\pi(i-1)n}{N}\right)-\cos\left(\frac{2\pi in}{N}\right)}{\pi n}\right)\cdot\left(\cos\left(\frac{2\pi(j-1)n}{N}\right)-\cos\left(\frac{2\pi jn}{N}\right)\right),$$
$$i,j=1,...,N;\quad i\ne j \tag{35}$$

We can observe that the relations (32), (33) and (34) are the maximum amount of information that we can get from the boundary conditions (12) because the right members of these relations are, except by the factor $1/\pi$, the Fourier coefficients of $V_2^{(i)}(R_1,\theta)$ with respect to the trigonometric system in $L_2(0,2\pi)$. Similarly (35) is the maximum of information that we can obtain from the data (16).

Relation (32) - (35) suggest the following problem:

### 3.1.2 Problem 1

For each fixed $i = 1,\ldots,N$, we have to solve the linear $(N-1)\times(N-1)$ system:

$$B_o^{(i)} + \sum_{n=1}^{(N-2)/2}\Big\{\Big(\sin\Big(\tfrac{2\pi jn}{N}\Big) - \sin\Big(\tfrac{2\pi(j-1)n}{N}\Big)\Big)A_n^{(i)} + \Big(\cos\Big(\tfrac{2\pi(j-1)n}{N}\Big) - \cos\Big(\tfrac{2\pi jn}{N}\Big)\Big)B_n^{(i)}\Big\} = c_{i,j}\,, \quad j = 1,\ldots,N;\quad j \neq i \tag{36}$$

After obtaining

$$B_o^{(i)},\ A_n^{(i)},\ B_n^{(i)},\ n = 1,\cdots,\frac{N-2}{2},\ i = 1,\cdots,N\,,$$

we compare the obtained values with the corresponding coefficients in (35) for $n = 1,\cdots,\dfrac{N-2}{2}$, and using (32), (33) and (34) we have:

$$b_o^{(i)} = \frac{N}{2\pi}B_o^{(i)}, \quad a_o^{(i)} = \frac{1}{N} - \frac{N}{2\pi}B_o^{(i)}\ln R_2, \tag{37}$$

$$a_n^{(i)} = \frac{1}{2R_2^n}\left\{A_n^{(i)} + \frac{\sin\Big(\tfrac{2\pi in}{N}\Big) - \sin\Big(\tfrac{2\pi(i-1)n}{N}\Big)}{\pi n}\right\} \tag{38}$$

$$c_n^{(i)} = \frac{1}{2R_2^n}\left\{B_n^{(i)} - \frac{\cos\Big(\tfrac{2\pi in}{N}\Big) - \cos\Big(\tfrac{2\pi(i-1)n}{N}\Big)}{\pi n}\right\} \tag{39}$$

$$b_n^{(i)} = \frac{R_2^n}{2}\left\{\frac{\sin\Big(\tfrac{2\pi in}{N}\Big) - \sin\Big(\tfrac{2\pi(i-1)n}{N}\Big)}{\pi n} - A_n^{(i)}\right\} \tag{40}$$

$$c_n^{(i)} = \frac{R_2^n}{2}\left\{\frac{\cos\Big(\tfrac{2\pi(i-1)n}{N}\Big) - \cos\Big(\tfrac{2\pi in}{N}\Big)}{\pi n} - B_n^{(i)}\right\} \tag{41}$$

Using these coefficients in equation (31), we obtain an approximation of $V_2^{(i)}(R_1,\theta)$ and $\dfrac{\partial V_2^{(i)}}{\partial n_1}(R_1,\theta)$, taking the sum from $n = 1$ to $n = \dfrac{N-2}{2}$.

Observe that in this way we obtain the best approximation of $V_2^{(i)}(R_1,\theta)$ and $\dfrac{\partial V_2^{(i)}}{\partial n_1}(R_1,\theta)$ as a linear combination of the trigonometric system using only the information from the boundary condition (12) and the data (16).

### 3.1.3 Step 2

We will use the expressions (23), (25) and (26) to calculate simultaneously $V_1^{(i)}$ and $\nabla V_1^{(i)}$.

From (23) we conclude that $V_1^{(i)}$ must be in such way that if $z = (x,y)$, $\xi = R_1 e^{i\tau}$, then

$$\frac{\partial V_1^{(i)}}{\partial y}(z)\cdot\int_{|\xi|=R_1}\frac{\partial V_2^{(i)}}{\partial n_1}(\xi)\frac{x - R_1\cos\tau}{|\xi - z|^2}\,ds_\xi = \frac{\partial V_1^{(i)}}{\partial x}(z)\cdot\int_{|\xi|=R_1}\frac{\partial V_2^{(i)}}{\partial n_1}(\xi)\frac{y - R_1\sin\tau}{|\xi - z|^2}\,ds_\xi \tag{42}$$

Let us find the vector function $\vec{V}_1 = (V_1^{(1)},\cdots V_1^{(N)})$ in some class of functions $\vartheta$ such that it minimizes the functional

$$l(\vec{V}_1) = \sum_{i=1}^{N}\left\{\left\|f_i(z)\frac{\partial V_1^{(i)}}{\partial y}(z) - g_i(z)\frac{\partial V_1^{(i)}}{\partial x}(z)\right\|^2 + \left\|V_1^{(i)}(z) - \int_{|\xi|<R_1}\nabla_\xi V_1^{(i)}(\xi)\cdot\nabla_\xi d(z,\xi)d\xi - F_i(z)\right\|^2 + \left\|V_1^{(i)}(z) - \int_{|\xi|<R_1}\nabla_\xi V_1^{(i)}(\xi)\cdot\nabla_\xi n(z,\xi)d\xi - G_i(z)\right\|^2\right\} \tag{43}$$

where the functions

$$f_i(z) = \int_{|\xi|=R_1}\frac{\partial V_2^{(i)}}{\partial n_1}(\xi)\frac{x - R_1\cos\tau}{|\xi - z|^2}\,ds_\xi \tag{44}$$

$$g_i(z) = \int_{|\xi|=R_1}\frac{\partial V_2^{(i)}}{\partial n_1}(\xi)\frac{y - R_1\sin\tau}{|\xi - z|^2}\,ds_\xi \tag{45}$$

$$F_i(z) = \int_{|\varphi|=R_1}F(z,\varphi)\frac{\partial V_2^{(i)}}{\partial n_1}(\varphi)ds_\varphi + h_i(z) \tag{46}$$

$$G_i(z) = \int_{|\varphi|=R_1}G(z,\varphi)\frac{\partial V_2^{(i)}}{\partial n_1}(\varphi)ds_\varphi + a_i \tag{47}$$

The functions $F(z,\varphi)$, $G(z,\varphi)$, $h_i(z)$ and the numbers $a_i$ are defined by (27) - (30). The norm considered in the functional (43) is the norm in $H^1(|z| < R_1)$.

From the fact that $\varepsilon_1(x,y)$ are lower-bounded by a strictly positive constant, it is easy to see that $V_1^{(i)} \in H^1(|z| < R_1)$. For that reason we look for $V_1^{(i)}$ in the form

$$V_1^{(i)}(z) = \sum_{k=1}^{M}a_k^{(i)}W_k(z) \tag{48}$$

where $\{W_k(z)\}_{k=1}^{\infty}$ is an orthonormal basis in $H^1(|z| < R_1)$ and the number $M$ will be chosen latter.

Putting the expression (48) in the functional (43), we obtain a new functional that depends on the

unknown values $a_k^{(i)}$, $k=1,\cdots,M$; $i=1,\cdots,N$ in (48):

$$L(a_k^{(i)}) = \sum_{i=1}^{N}\sum_{j=1}^{M}\left\{\left|\sum_{k=1}^{M} a_k^{(i)} f_{jk}^{(i)}\right|^2 + \left|\sum_{k=1}^{M} a_k^{(i)} D_{jk} - F_j^{(i)}\right|^2 + \left|\sum_{k=1}^{M} a_k^{(i)} N_{jk} - G_j^{(i)}\right|^2\right\} \quad (49)$$

If we suppose that $\varepsilon_1(x,y)$ satisfies $0<\varepsilon_{\min}\le\varepsilon_1(x,y)\le\varepsilon_{\max}$, then from (23) we obtain $2N$ restrictions for the unknown coefficients $a_k^{(i)}$, which give origin to the following problem:

### 3.1.4 Problem 2(i) (*i* = 1,…,*N*)

Find the minimum of the quadratic functional

$$\left|F_i\vec{a}_i\right|_M^2 + \left|D\vec{a}_i - \vec{b}_i\right|_M^2 + \left|N\vec{a}_i - \vec{c}_i\right|_M^2 \quad (50)$$

subject to the restrictions

$$\frac{\varepsilon_2 R_1}{\sqrt{2\pi}\varepsilon_{\max}} \le \left|A_i\vec{a}_i\right|_M \le \frac{\varepsilon_2 R_1}{\sqrt{2\pi}\varepsilon_{\min}} \quad (51)$$

$$\frac{\varepsilon_2 R_1}{\sqrt{2\pi}\varepsilon_{\max}} \le \left|B_i\vec{a}_i\right|_M \le \frac{\varepsilon_2 R_1}{\sqrt{2\pi}\varepsilon_{\min}} \quad (52)$$

where $|\cdot|_M$ denotes the Euclidean norm of a vector in $R^M$, $F_i=\left(f_{jk}^{(i)}\right)$, $A_i=(\alpha_{jk}^{(i)})$, $B_i=(\beta_{jk}^{(i)})$, $D=(D_{jk})$ y $N=(N_{jk})$ are matrices of order $M\times M$, where $1\le j,k\le M$, $i=1,\cdots,N$. The coefficients $f_{jk}^{(i)}$, $D_{jk,}$, $N_{jk}$ are the Fourier coefficients in $H^1(|z|<R_1)$ of the functions

$$f_i(z)\frac{\partial W_k}{\partial y}(z) - g_i(z)\frac{\partial W_k}{\partial x}(z)$$

$$W_k(z) - \int_{|\xi|<R_1}\nabla_\xi W_k(\xi)\cdot\nabla_\xi d(z,\xi)d\xi - F_i(z) \text{ and}$$

$$W_k(z) - \int_{|\xi|<R_1}\nabla_\xi W_k(\xi)\cdot\nabla_\xi n(z,\xi)d\xi - G_i(z)$$

with respect to the orthonormal system $\{W_j(z)\}_{j=1}^{M}$.

This basis can be taken in such a way that for some coefficients $\gamma_j$ we have that $\{\gamma_j W_j(z)\}_{j=1}^{\infty}$ is an orthonormal basis in $L_2(|z|<R_1)$ [4]. Therefore, $\alpha_{jk}^{(i)}$ and $\beta_{jk}^{(i)}$ are the Fourier coefficients in $L_2(|z|<R_1)$ of the functions $\frac{1}{f_i(z)}\frac{\partial W_j}{\partial x}(z)$ and $\frac{1}{g_i(z)}\frac{\partial W_j}{\partial y}(z)$, respectively, with respect to the orthonormal system $\{\gamma_j W_j(z)\}_{j=1}^{M}$, where $f_i(z)$ and $g_i(z)$ are defined by (44) and (45).

Finally, $\vec{a}_i$, $\vec{b}_i$, $\vec{c}_i$ denote the vectors

$$\vec{a}_i=\begin{pmatrix}a_1^{(i)}\\a_2^{(i)}\\\vdots\\a_M^{(i)}\end{pmatrix},\quad \vec{b}_i=\begin{pmatrix}F_1^{(i)}\\F_2^{(i)}\\\vdots\\F_M^{(i)}\end{pmatrix},\quad \vec{c}_i=\begin{pmatrix}G_1^{(i)}\\G_2^{(i)}\\\vdots\\G_M^{(i)}\end{pmatrix}$$

where $F_j^{(i)}$ and $G_j^{(i)}$ are the Fourier coefficients in $H^1(|z|<R_1)$ of the functions $F_i(z)$ and $G_i(z)$, defined by (46) and (47), with respect to the orthonormal system $\{W_j(z)\}_{j=1}^{M}$.

In order to obtain the solution of the problem (2i) in a numerically stable form, we must apply some regularization algorithm (this will be the subject of future works).

### 3.1.5 Step 3

When the problems 1 and (2i) are solved, we obtain approximate values for $\frac{\partial V_2^{(i)}}{\partial n_1}(\xi)$ in $|\xi|=R_1$ and $\nabla V_1^{(i)}(z)$ in $|z|<R_1$.

Using expression (23) we can obtain the approximation to $\varepsilon_1(x,y)$. So that this expression will not depend on $i=1,\cdots,N$, we will suppose that

$$\varepsilon_1(z) = \frac{\varepsilon_2}{\pi N}\sum_{i=1}^{N}\frac{\left|\int_{|\xi|=R_1}\frac{\partial V_2^{(i)}}{\partial n_1}(\xi)\nabla_z\ln|z-\xi|ds_\xi\right|}{\left|\nabla V_1^{(i)}(z)\right|} \quad (53)$$

If we have the partition $(\omega_k)_{k=1}^{\tilde{M}}$ of $|z|<R_1$, then expression (53) can be used to obtain an average value $\varepsilon_1^k$ of $\varepsilon_1(x,y)$ for each element of the partition.

It is possible to prove that we can take $M=\tilde{M}$ and equal to the maximum number of elements of the partition in which each component $\omega_k$ is that the change of $\varepsilon_1^k$ in $\omega_k$ can be detected by the instrument used to measure the mutual capacitances.

## 4 Conclusion

Obviously the function $V_2^{(i)}$ depends implicitly in nonlinear way on the unknown permittivity $\varepsilon_1(x,y)$, and, therefore, obtaining $\varepsilon_1(x,y)$ from the measurements (16) consists formally in solving the nonlinear equation

$$A(\varepsilon_1) = \vec{C}$$

where the $A$ operator acts on a space of functions defined in $\Omega_1$ and takes the values on $R^{N(N-1)/2}$.

The general method to solve this kind of problem is to discretize the operator $A$ into an operator $\tilde{A}$ acting in $R^{N(N-1)/2}$ on itself, and after that minimizing the functional

$$\left\| \tilde{A}(\tilde{\varepsilon}_1) - \vec{C}_{obs} \right\| \qquad (54)$$

on a set vectors $\tilde{\varepsilon}_1$ that correspond to an approximate representation of the function $\varepsilon_1$, and where $\vec{C}_{obs}$ corresponds to the vector of data $\{c_{ij}\}$ obtained as a result of the measurements of the mutual capacitance and the formulas (15) and (16) (see [1], [6], [7], [8], [9]).

The problem in considering the functional (54) is that it is a nonlinear functional that can have multiple extreme points, and, according to (14), (15) and (16), in the definition of $\tilde{A}$ appears implicitly an ill-posedness due to the derivatives of $V_2^{(i)}$ involved in the definition of $\{c_{ij}\}$, and it is well known that the process of derivation is an ill-posed problem and numerically unstable.

To avoid these difficulties we have developed an algorithm in which the problem of identification of $\varepsilon_1(x,y)$ reduces to the solution of linear systems equations and least-squares problems with quadratic restrictions.

The advantages of this method with respect to the traditional minimization of the nonlinear functional (54) are the following

- The traditional method is fully iterative, while in the proposed direct method we have to do some calculations only one time.
- The proposed procedure allows calculating the accumulated error in each step more efficiently. This error is composed basically of the truncation error that we have when we approximate the series by a partial sum, plus the error coming from the measured data.
- In the nonlinear functional case (54), the regularization techniques employed have only an empiric character, because there are no theoretical results applicable.

*References:*


[1] M. Cheney, D. Isaacson, An overview of inversion algorithms for impedance imaging, *Contemporary Mathematics*, vol 122, (1991), 29-39.

[2] Hammer E.A., Johansen G.A., Process Tomography in the oil industry: state of the art and future possibilities, *Measurement and Control*, Vol 30, September (1997), 212-216.

[3] Kirsh A., *An Introduction to the Mathematical Theory of Inverse Problems*, AMS 120, Springer, New York, 1996.

[4] Mijailov V. P., *Ecuaciones Diferenciales en derivadas parciales*, Mir-Moscow, 1982.

[5] Ostrowski K. L., Luke S. P., Williams R. A., Application of conjugate harmonics to electrical process tomography. *Meas. Sci. Technol.*, 7, (1996), 316-324.

[6] Spink D.M., Noras J. M., Recent development in the solution of the forward problem in capacitance tomography and implications for iterative reconstruction, *GPA*, India, (1998), 115-142.

[7] Thorn R., Johansen G. A., Hammer E. A. Recent developments in three-phase flow measurement, *Measurement Science and Technology*, 8, (1997), 691-701.

[8] Xie C.G., Plaskoswki, Beck M.S., 8-electrode capacitance system for two component flow identification. Part 1.: Tomographic flow imaging, *IEE Proceedings Pt. A*, Vol. 136, No.4 (1989), 173-183.

[9] Xie C. G., Huang S. M., et al., Electrical Capacitance Tomography for flow imaging: System model for development of image reconstruction algorithm and design of primary sensors. *IEE Proceedings G*, Vol. 139, No.1 (1992), 89-98.

[10] Yang W. Q., Beck M.S., Byars M., Electrical Capacitance Tomography: from design to applications, *Measurement and Control*, 28, (1995), 261-266.

[11] Yang W. Q., Stott A. L., Xie C. G., Beck M. S., Development of Capacitance Tomographic Imaging System for oil Pipeline Measurements, *Review of Scientific Instruments*, (1995) 66 4326-4332.